The Dynamic Mechanism of the Formation of the Low Level Jet

Yang Dasheng (杨大升) and *Jian Maoqiu* (简茂球)
Department of Geophysics, Peking University, Beijing 100871
Received February 22, 1990

ABSTRACT

The ordinary multidimensional reductive perturbation method is generalized so as to apply to the general case including the dissipative factor. With this the corresponding Cubic–Schrödinger equation is deduced, and by the preliminary study of its solution, it shows that it is more admissible to consider atmospheric meso–scale systems as the nonlinear Cubic–Schrödinger waves.With suitable boundary and initial conditions, the Cubic–Schrödinger equation is numerically integrated so as to investigate the possible dynamic mechanism as well as the impacts of the nonlinear action, turbulent friction and topogrphy to the formation of the LLJ. The results indicate that the downward transfer of the momentum and the effect of the surface friction are responsible for the concentration of the momentum in the layer between 850 and 700 hPa. The location of the horizontal concentration of momentum depends on the propagation of momentum, in the process the inertia–gravity internal wave is very important, whereas turbulent friction is unfavourable for or delays the formation of the low level jet.

I. INTRODUCTION

Low level Jet (abbreviated to LLJ) is recognized as the most important and frequent synoptic system of the severe rain in China, causing heavy losses and frustration in the human activity and economic construction. In recent decades there are a large amount of synoptic and dynamic studies (Ninomiya et al., 1974; Hart, 1977; Synoptic Section of TOMI of Guangdong Province, 1977; Uccellini et al., 1979; Chen ,1982; Yang, 1983; Gao et al., 1984; Yang and Zhang,1984) on its genesis, structure, dynamic mechanism and weather significance as well as process. But most of the works are concentrated on the linear analysis. So far as we know the LLJ is rather a mesoscale system, thus the non–linear effect can not be ignored. In this investigation, we make a preliminary study on the dynamic mechanism of the formation of the LLJ in terms of he nonlinear interaction.

II. GOVERNING EQUATION AND THE 2–DIMENSIONAL CUBIC SCHRODINGER EQUATION

Choose x axis as along the LLJ, along which all meteorological elements or variables are considerably uniform, thus the governing equations are

$$\frac{\partial u}{\partial t}+v\frac{\partial u}{\partial y}+\frac{w\partial u}{\partial z}-fv=A_H\frac{\partial^2 u}{\partial y^2}+A_v\frac{\partial^2 u}{\partial z^2} \tag{1}$$

$$\frac{\partial v}{\partial t}+v\frac{\partial v}{\partial y}+w\frac{\partial v}{\partial z}+fu=-\frac{1}{\rho}\frac{\partial P}{\partial y}+A_H\frac{\partial^2 v}{\partial y^2}+A_v\frac{\partial^2 v}{\partial z^2} \tag{2}$$

$$\frac{\partial w}{\partial t}+v\frac{\partial w}{\partial y}+w\frac{\partial w}{\partial z}=-\frac{1}{\rho}\frac{\partial P}{\partial z}+A_H\frac{\partial^2 w}{\partial y^2}+A_v\frac{\partial^2 w}{\partial z^2}-g \tag{3}$$

$$\frac{\partial T}{\partial t}+v\frac{\partial T}{\partial y}+w\frac{\partial T}{\partial z}+\sigma w=0 \tag{4}$$

$$\frac{\partial v}{\partial y}+\frac{\partial w}{\partial z}+\frac{1}{\rho_0}\frac{\partial \rho_0}{\partial z}w=0 \tag{5}$$

In which $\sigma=g/c_p$, the adiabatic lapse rate, and equation (4) expresses the first law of thermodynamics for adiabatic process. A_H, A_v are respectively the horizontal and vertical kinematic eddy viscous coefficient. $\rho_0(z)$ is the air density in the basic state, which with other basic state quantities $P_0(z)$, $\overline{T}(z)$ are functions of z only. Other symbols are as usually used in atmospheric sciences. Suppose, θ, p' and ρ' are separately the perturbed temperature, pressure and density. Further assume

$$\nabla p'=\rho_0\beta\nabla\theta \tag{6}$$

where β is a parameter yet to be determined. When inserting θ and Eq.(6) into Eqs.(1)–(5), then we get the following equations for studying the LLJ,

$$\frac{\partial u}{\partial t}+v\frac{\partial u}{\partial y}+w\frac{\partial u}{\partial z}-fv=A_H\frac{\partial^2 u}{\partial y^2}+A_v\frac{\partial^2 u}{\partial z^2} \tag{1}$$

$$\frac{\partial v}{\partial t}+v\frac{\partial v}{\partial y}+w\frac{\partial v}{\partial z}+fu=-\frac{1}{\rho_0}\frac{\partial P'}{\partial y}+A_H\frac{\partial^2 v}{\partial y^2}+A_v\frac{\partial^2 v}{\partial z^2} \tag{7}$$

$$\frac{\partial w}{\partial t}+v\frac{\partial w}{\partial y}+w\frac{\partial w}{\partial z}=-\frac{1}{\rho_0}\frac{\partial P'}{\partial z}+\frac{\theta}{\overline{T}}+A_H\frac{\partial^2 w}{\partial y^2}+A_v\frac{\partial^2 w}{\partial z^2} \tag{8}$$

$$\frac{\partial \theta}{\partial t}+v\frac{\partial \theta}{\partial y}+w\frac{\partial \theta}{\partial z}+dw=0 \tag{9}$$

$$\frac{\partial v}{\partial y}+\frac{\partial w}{\partial z}-N^2w=0 \tag{10}$$

Where $d=\sigma+\frac{d\overline{T}(z)}{dz}$, $N^2=-\frac{1}{\rho_0}\frac{d\rho_0}{dz}$. The above former four equations can be put into the following matrix form

$$\frac{\partial \tilde{U}}{\partial t}+\tilde{A}_i\frac{\partial \tilde{U}}{\partial x_i}+\tilde{B}+\tilde{C}_i\frac{\partial^2 \tilde{U}}{\partial x_i^2}=0 \tag{11}$$

In which suffix $i=1,2$ denoting directions along y and z coordinates respectively and the summation convention for index i is implied. Moreover, $x_1=y$, $x_2=z$;

$$\tilde{U}=\begin{bmatrix} u \\ v \\ w \\ \theta \end{bmatrix};\qquad \tilde{B}=\begin{bmatrix} -fv \\ fu \\ -\frac{g}{\overline{T}}\theta \\ dw \end{bmatrix};$$

$$\tilde{A}_1\begin{bmatrix} v & 0 & 0 & 0 \\ 0 & v & 0 & \beta \\ 0 & 0 & v & 0 \\ 0 & 0 & 0 & v \end{bmatrix}; \qquad \tilde{C}_1 = \begin{bmatrix} -A_H & 0 & 0 & 0 \\ 0 & -A_H & 0 & 0 \\ 0 & 0 & -A_H & 0 \\ 0 & 0 & 0 & 0 \end{bmatrix}, \tag{12}$$

$$\tilde{A}_2\begin{bmatrix} w & 0 & 0 & 0 \\ 0 & w & 0 & 0 \\ 0 & 0 & w & \beta \\ 0 & 0 & 0 & w \end{bmatrix} \qquad \tilde{C}_2 = \begin{bmatrix} -A_v & 0 & 0 & 0 \\ 0 & -A_v & 0 & 0 \\ 0 & 0 & -A_v & 0 \\ 0 & 0 & 0 & 0 \end{bmatrix},$$

Evidently, equation (11) admits constant solution $\tilde{U}^{(0)}$, $\tilde{U}^{(0)} = (0\ 0\ 0\ 0)'$, thus $\tilde{B}^{(0)} = \tilde{B}(\tilde{U}^{(0)}) = 0$, and the linearized equation (11) with respect to $\tilde{U}^{(0)}$ takes the form

$$\frac{\partial \tilde{U}}{\partial t} + \tilde{A}_i^{(0)}\frac{\partial \tilde{U}}{\partial x_i} + \nabla \tilde{B}^{(0)}\tilde{U} + \tilde{C}_i^{(0)}\frac{\partial^2 \tilde{U}}{\partial x_i^2} = 0\ , \tag{13}$$

where $\tilde{A}_i^{(0)}$, $\tilde{C}_i^{(0)}$ are the $\tilde{A}_i$, $\tilde{C}_i$ matrix calculated with $\tilde{U}^{(0)}$, whereas

$$(\nabla \tilde{B}^{(0)})_{ij} = \left(\frac{\partial \tilde{B}_i}{\partial u_j}\right)_{U-U^{(0)}}$$

Substitution of the following expression into (13)

$$\tilde{U} \sim \exp i(k_i x_i - \omega t) \tag{14}$$

where $k_i (i = 1,2)$ are the wave numbers along x_i directions, and ω is the complex frequency, yields

$$|W_1| = \left| -i\omega \vec{I} + ik_i \tilde{A}_i^{(0)} - \nabla \tilde{B}^{(0)} - k_i^2 \tilde{C}_i^{(0)} \right| = 0 \tag{15}$$

In which, $\vec{I}$ is the unit vector.

From (15), ω is determined by

$$\omega^4 + \omega^2 d(ik_2\beta - \gamma g) - f^2\omega^2 - f^2 d(ik_2\beta - \gamma g) = 0 \tag{16}$$

where $\gamma = \frac{1}{T}$. The above equation (11) is solved by reductive perturbation method, by which the sophisticated nonlinear equation system describing the nonliear wave is reduced to a unique simple and soluble nonlinear equation. It is carried out by means of Gardner–Morikawa transformation and the general perturbation method. The G–M transformation is as follows,

$$\xi_i = \varepsilon(x_i - \lambda_i^{(0)} t), \quad \tau = \varepsilon^2 t \quad (i = 1,2) \tag{17}$$

ε is a small parameter, λ_i is the group velocity in the x_i direction, and

$$\lambda_i = \lambda_i^{(0)} + \varepsilon \tilde{U}^{(1)}(\nabla_u \lambda_i)_{U^{(0)}} = \lambda_i^{(0)} + \varepsilon \sum_{j=1}^{4} u_j^{(1)} \left(\frac{\partial \lambda_i}{\partial u_j}\right)_{U^{(0)}} \tag{18}$$

$\tilde{U}$ is a symptotically expanded in power series of ε as follows,

$$\tilde{U} = \sum_{\alpha=0}^{\infty} \varepsilon^{\alpha} \tilde{U}^{(\alpha)} \tag{19}$$

$$\tilde{U}^{(\alpha)} = \sum_{l=-\infty}^{\infty} \tilde{U}_l^{(\alpha)}(\xi_i,\tau) e^{il(k_i x_i - \omega t)} \tag{20}$$

Since $\tilde{U}^{(\alpha)}$ is real, thus it is necessary that $\tilde{U}_l^{(\alpha)} = \tilde{U}_{-l}^{(\alpha)*}$. Because here we only consider the modulation of the plane wave with frequency ω and wave number k, hence we assume for $l \neq \pm 1$,

$$\tilde{U}_l^{(1)} = 0 \tag{21}$$

In addition, $\tilde{A}_i$, $\tilde{B}$ and $\tilde{C}_i$ in (11) can be expanded as

$$\tilde{A}_i = \tilde{A}_i^{(0)} + \varepsilon \nabla \tilde{A}_i^{(0)} \tilde{U}^{(1)} + \varepsilon^2 \left(\nabla \tilde{A}_i^{(2)} + \frac{1}{2} \nabla\nabla \tilde{A}_i^{(0)} : \tilde{U}^{(1)} \tilde{U}^{(1)} \right) + \cdots \tag{22}$$

$$\tilde{B} = \tilde{B}^{(0)} + \varepsilon \nabla \tilde{B}^{(0)} \tilde{U}^{(1)} + \varepsilon^2 \left(\nabla \tilde{B}^{(2)} + \frac{1}{2} \nabla\nabla \tilde{B}^{(0)} : \tilde{U}^{(1)} \tilde{U}^{(1)} \right) + \cdots \tag{23}$$

$$\tilde{C}_i = \tilde{C}_i^{(0)} + \varepsilon \nabla \tilde{C}_i^{(0)} \tilde{U}^{(1)} + \varepsilon^2 \left(\nabla \tilde{C}_i^{(2)} + \frac{1}{2} \nabla\nabla \tilde{C}_i^{(0)} : \tilde{U}^{(1)} \tilde{U}^{(1)} \right) + \cdots \tag{24}$$

where

$$\nabla \tilde{A}_i^{(0)} \tilde{U}^{(1)} = \left(\frac{\partial \tilde{A}_i}{\partial u_i} \right)_{\tilde{V}^{(0)}} u_j^{(1)}; \quad \nabla\nabla \tilde{A}_i^{(0)} : \tilde{U}^{(1)} \tilde{U}^{(1)} = \left(\frac{\partial^2 \tilde{A}_i}{\partial u_j \partial u_k} \right)_{\tilde{V}^{(0)}} u_j^{(1)} u_k^{(1)}$$

Replacing (19), (20), (22)–(24) into the G–M transformed equation (11), then comparing the terms with same power of ε, we get the equation of various order of approximation for solving $\tilde{U}_l^{(\alpha)}(\xi_i,\tau)$. Among which the equation for the ε order of approximation is

$$\tilde{W}_l \tilde{U}_l^{(1)} = 0 \tag{25}$$

where $\tilde{W}_l$ stands for the matrix $-il\omega\vec{I} + ilk_i \tilde{A}_i^{(0)} + \nabla \tilde{B}^{(0)} - k_i^2 l^2 \tilde{C}_i^{(0)}$.

In virtue of equation (15), we can assume in general

$$\det \tilde{W}_l \neq 0 \qquad \text{for } |l| \neq 1 \tag{26}$$

Equation (26) also leads to the conclusion (21).

From equations (15) and (25), then for $|l| = 1$,

$$\tilde{U}_l^{(1)} = \varphi(\xi_i,\tau)\tilde{R}, \qquad \tilde{U}_{-l}^{(1)} = \varphi^* \tilde{R}^* \tag{27}$$

In which $\tilde{R} = (r_1, r_2, r_3, r_4)^T$ is the right characteristic vector of $\tilde{W}_1$ corresponding to the eigenvalue zero. Then from $\tilde{W}_l \tilde{R} = 0$, we obtain

$$\tilde{R}=\begin{bmatrix} r_1 \\ r_2 \\ r_3 \\ r_4 \end{bmatrix} \propto \begin{bmatrix} fk_1\beta\omega \\ -ik_1\beta\omega^2 \\ (f^2-\omega^2)(ik_2\beta-\gamma g) \\ i\omega(f^2-\omega^2) \end{bmatrix} \tag{28}$$

With the aid of equation (27), also the perturbed field satisfies continuity equation (10), thus the undetermined parameter β is given by

$$i\beta=\frac{\gamma g(k_2-N^2)(f^2-\omega^2)}{-k_i^2\omega^2+k_2(k_2-N^2)(f^2-\omega^2)} \tag{29}$$

Inserting (29) into (16), then

$$\omega_{1,2}=\pm f \tag{30}$$

$$\omega_{3,4}=\pm[(k_2(k_2-N^2)f^2+d\gamma g k_1^2)/(k_1^2+k_2(k_2-N^2))]^{1/2} \tag{31}$$

Evidently, ω has real roots. $\omega_{1,2}$, are the frequencies of the pure inertial wave, which can be ignored, whereas $\omega_{3,4}$ are that of the relatively important inertia–gravity internal waves, which play the fundamental role in the process of LLJ.

For the problem of LLJ, $|\nabla\tilde{B}^{(0)}|\neq 0$, according to (29), β is a pure imaginary number, since ω possesses real value, thus the conjugate vector to $\tilde{R}'$ (transposition of $\tilde{R}$, i.e.expression (28)) is

$$R^*=(-fk_1\beta\omega,-ik_1\beta\omega^2,(f^2-\omega^2)(ik_2\beta-\gamma g),-i\omega(f^2-\omega^2)) \tag{32}$$

Let L be the left characteristic vector of $\tilde{W}_1$, then since $\det|\tilde{W}_1|=0$, $\tilde{L}\tilde{W}_1=0$, which yields

$$L=(0,0,d,i\omega) \tag{33}$$

By using the equation of the ε^2 order of approximation, the following relations are obtained,

$$\tilde{U}_0^{(2)}=\tilde{R}_0^{(2)}|\varphi|^2 \tag{34}$$

$$\tilde{U}_1^{(2)}=\tilde{R}\varphi'-i\frac{\partial(\tilde{R}\varphi_{\xi i})}{\partial k_i} \tag{35}$$

$$\tilde{U}_2^{(2)}=\tilde{R}_2^{(2)}\varphi^2 \tag{36}$$

$$\tilde{U}_{-2}^{(2)}=\tilde{R}_{-2}^{(2)}(\varphi^*)^2 \tag{37}$$

and

$$\tilde{U}_l^{(2)}=0, \quad \text{for} \quad |l|\geqslant 3 \tag{38}$$

where $\tilde{R}_0^{(2)}$, $\tilde{R}_2^{(2)}$ and $\tilde{R}_{-2}^{(2)}$, are coefficients consisting of k_i, $\nabla\tilde{A}_i^{(0)}$, $\nabla\nabla\tilde{B}^{(0)}$, $\nabla\tilde{C}_i^{(0)}$ and $\tilde{R}$ operated with $\tilde{W}_0^{-1}$, $\tilde{W}_2^{-1}$ and $(\tilde{W}_0^*)^{-1}$ respectively.

By using the equation of ε^3 order of approximation, the matrix equation (11) is finally reduced to a unique scalar equation for the single variable $\varphi(\xi_i,\tau)$, which runs as follows,

$$i\varphi_\tau + b_{ij}^* \varphi_{\xi_i \xi_j} + C^* |\varphi|^2 \varphi + id^* \varphi = 0 \tag{39}$$

This is the generalized 2-dimensional cubic-Schrodinger equation, in which, the dependent variable $\varphi(\xi_i, \tau)$ modulates the slow variations in space and time, and

$$b_{ij}^* = \frac{1}{2} \frac{\partial^2 \omega}{\partial k_i \partial k_j} \tag{40}$$

$$c^* = \frac{3N^4(-\omega^2 + d\gamma g)}{d^2(2\omega^2 + d\gamma g)} \omega^3 (\omega^2 - f^2)^2 \tag{41}$$

$$d^* = \frac{i}{2} \varepsilon^{-2} (k_1^2 A_H + k_2^2 A_v) \tag{42}$$

III. IMPACT OF NONLINEARITY, TURBULENT FRICTION AND TOPOGRAPHY ON THE FORMATION OF LLJ

For the convenience of numerical integration of (39), we first make the following transformation,

$$\begin{aligned} \eta_1 &= \xi_1 + l_1 \tau, \quad l_1 = \frac{\lambda_1^{(0)}}{\varepsilon} \\ \eta_2 &= \xi_2 + l_2 \tau, \quad l_2 = \frac{\lambda_2^{(0)}}{\varepsilon} \\ \tau &= \tau \end{aligned} \tag{43}$$

Replacing (43) into (39), then

$$\begin{aligned} \frac{\partial \varphi}{\partial \tau} - ib_{11}^* \frac{\partial^2 \varphi}{\partial \eta_1^2} - 2ib_{12}^* \frac{\partial^2 \varphi}{\partial \eta_1 \partial \eta_2} - ib_{22}^* \frac{\partial^2 \varphi}{\partial \eta_2^2} + \frac{\lambda_1^{(0)}}{\varepsilon} \frac{\partial \varphi}{\partial \eta_1} \\ + \frac{\lambda_2^{(0)} \partial \varphi}{\varepsilon \partial \eta_2} + d^* \varphi - ic^* |\varphi|^2 \varphi = 0 \end{aligned} \tag{44}$$

The numerical integration of (44) is accomplished by the alternate ADI method.

When φ field is obtained, then from the relations of u, v, w and T, to φ expressed by(27), (34), (35), (36) and (37), we get the numerical values of u, v, w, and T consequently.

The following values are preassigned for the parameters

$$\begin{aligned} &L_y = 4000\text{km}, \ L_x = 20\text{km}, \ y = 0.001\text{k}^{-1}, \ g = 9.8\text{m/s}^2 \\ &d = \frac{g}{C_p} + \frac{\partial \overline{T}}{\partial z} = 1.3 \times 10^{-3}\text{k/m}, \ f = 2\Omega\sin 30^\circ = 7.29 \times 10^{-5}\text{s}^{-1}, \\ &N^2 = -\frac{1}{\rho_0} \frac{\partial p_0}{\partial z} = 1.5 \times 10^{-4}\text{m}^{-1}, \ A_H = 10^5\text{m}^2\text{s}^{-1}, \\ &A_v = 10\text{m}^2\text{s}^{-1} \ \text{(Pedlosky,1979)} \end{aligned} \tag{45}$$

Since the right characteristic vector $\tilde{R}$ to the linear dispersion matrix corresponds to the column vector $\tilde{U}$, it is interesting to note that from the expression of $\tilde{R}$, the two former components demonstrate when $\omega < f$, i.e. for low frequency disturbance, the magnitude of u

is larger than that of v, it is quite in accord with observation, because low frequency motion is usually chiefly along the direction of jet axis.

To integrate (44) numerically, time length for each step is set at $\Delta t = 60$s, space interval $\Delta y = 150$km, and $\Delta z = 1$km, which gives the total grid network 21×11. Homogeneous boundary conditions are assumed on the lower and upper boundary. On the left lateral boundary, the boundary values are determined by extrapolating the values from the outside neighbouring grid points, whereas on the right lateral bundary, the specified functions are assigned to the variables φ_r and φ_i (the real and imaginary part of φ),

$$\varphi_r = -A_0 \exp(-d\tau)\sin\theta$$
$$\varphi_i = A_0 \exp(-d\tau)\cos\theta \tag{46}$$

where A_0 is a constant, $\theta = (k_2 z - \omega t)$.

First, we experiment with an initial wind field as shown in Fig.1. On its left lower corner, there is a slanting topography of 2 km high and with a slope of 1 in 150. The positive y axis is from S to N. Evidently, at the initial instant, the maximum wind (both u and v are negative) centre is at the 7km level and on the lower level there are no strong wind centres. With increase of time, the centres of negative u,v component move downwards and to the left, when integrating to 14hr., low-level jet appears as shown in Figs.2 and 3. Hence it seems that the strong wind zone in the lower level is formed through the downward transfer of upper level momentum, in conjunction with the impedance on the lower boundary, so that the horizontal momentum is concentrated in the layer between heights of about 1.5 and 4 km. Moreover this downward tranfer is essentially accomplished by the inertia-gravity internal wave, this accords with the well known results that inertia-gravity internal wave contributes to the genesis and development of LLJ and heavy precipitation. Besides, as noted in Fig.3, the ascending motion coincides with the zone of strong negative u component in front of the sloped topography while the descending motion coincides with the zone of positive u component far away from the topography.

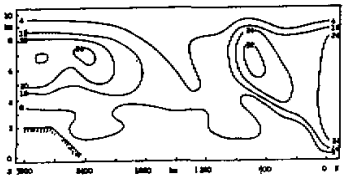

Fig.1. The y-z cross-section of initial total wind.unit: ms^{-1}.

However, the LLJ is sensitive to the initial wind fields, if the initial value of φ is set equal to zero, then the velocity field has the distribution of the pure sinusoidal function, and no LLJ can develop explicitly through integration.

In order to consider the impact of the nonlinearity, we omit the terms pertaining to eddy viscosity and topography. Taking the same initial value, the velocity fields integrated with and without nonlinear term (the cubic term in the generalized cubic-Schrodinger equation) are compared, which are depicted in Figs.4 with 5. Comparing Fig.4 with Fig.5, it is to be noted that u fields with and without nonlinear effect are different, the magnitude of u field with-

out nonlinear term is generally larger than that with nonlinear effect, this seems to diminish the magnitude of u component through nonlinearity. It is also evident on the figures that the downward propagation of the negative u component centre on the left part without nonlinear term is slower than that with nonlinear term. Nonetheless, with the positive u component centre on the right part the contrary is the case.

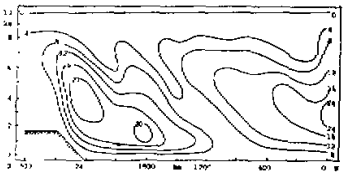

Fig.2. Total wind distribution at 14hr. unit: ms^{-1}.

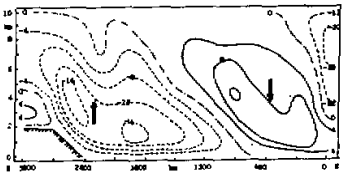

Fig.3. Distribution of u component at 14hr., dashedline—negative value; arrowed bar—assending or descending.

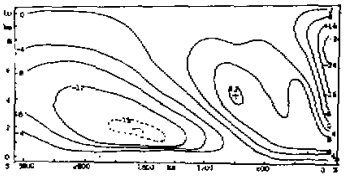

Fig.4 y—z cross section of u component at 14hr. with nonlinear term. unit: ms^{-1}.

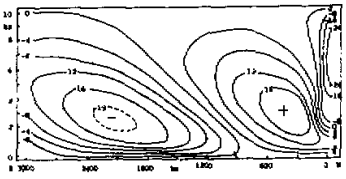

Fig.5. y—z cross section of u component at 14hr. without nonlinear term. unit: ms^{-1}.

It is worthy to remark that below 7km level nonlinear effect increases with time, as can be seen from Fig.6 and Fig.7.

For the purpose of gaining some concrete ideas about the influence of turbulent friction, we take different values of A_H, A_v to solve the frequency ω for the linear dispersion eqution (16) by an iterative method, the results are enumerated in Table 1. As can be seen from the table, when A_H and A_v increase, ω_r decreases in magnitude somewhat, whereas ω_i grows considerably. ω_r possesses negative value owing to the wave propagating in the opposite direction to the jet axis. This indicates that with the increase of the frictional effect, the wave velocity slows down, whereas the diminution of the amplitude becomes fast, besides, eddy viscosity has much greater effect on ω_i than on ω_r.

Table 1. Effect of Turbulent Friction on the Complex Frequency $\omega_r + i\omega_i$

A_H ($m^2\ s^{-1}$)	10^5	10^6	10^7
A_v ($m^2\ s^{-1}$)	10	10^2	10^3
ω_i (s^{-1})	-1.1976×10^{-6}	-1.1984×10^{-5}	-1.2228×10^{-4}
ω_r (s^{-1})	-7.5051×10^{-5}	-7.4982×10^{-5}	-7.3469×10^{-5}

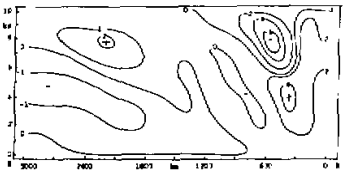

Fig.6. Difference of u component between with and without nonlinear term at 6hr. unit: ms^{-1}.

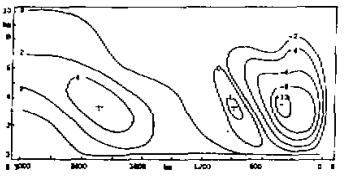

Fig.7. Same as Fig.6. except at 14hr.

We also integrate the velocity fields with the three pairs of value of A_H, A_v, as in Table 1 and with the same initial condition, and attain results as shown in Figs.8. and 9. From which it can be seen that with the increase of A_H, A_v, the centre of the maximum wind velocity displaces upward, its horizontal migration is obscure, and the magnitude of velocity diminishes notably. This is because that when A_H, A_V are getting larger, the wave velocity along $-z$ direction (downward) becomes slower, whereas that in $-y$ direction (toward left) has no corresponding reduction, then after 14hr the above phenomena occur. Therefore eddy viscosity is unfavorable for or delays the formation of the LLJ. This agrees with the results obtained by Hart (1977) that the larger the lateral eddy viscous coefficient, the farther is the peak value of the alongshore currents from the coast and the weaker is the amplitude of the current.

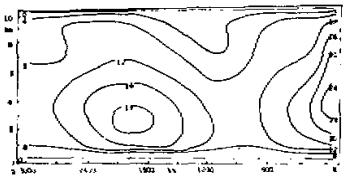

Fig.8. Distribution of the total wind velocity at 14 hr. with $A_H = A_V = 0$, in ms^{-1}.

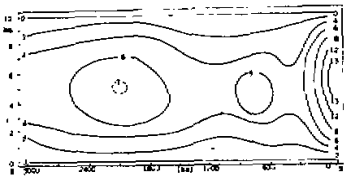

Fig.9. Same as Fig.8 except with $A_H = 10^5$ m^2s^{-1}, $A_V = 10$ m^2s^{-1}.

For studying the impact of the topography, we eliminate the nonlinear as well as the eddy viscous terms, and have run five experiments, that is: (1) no topography; (2) topography of

3 km in height, but slants to the right; (3) topography of 3km in height, with its right side vertical; (4) topography of 2 km in height, and slants to the right; (5) topography of 1 km in height, and slants to the right. All experiments are integrated to 12 hr. under the same initial condition.

Table 2. Topographic Effect on Low Level Jet ($Y=y$ Coordinate, Positive from Left to Right)

topography	(1)	(2)	(3)	(4)	(5)
height (km)	0	3 sloped	3 vertical	2 sloped	1 sloped
$\|u\|_{max}$ (ms^{-1})	19.71	23.56	25.03	22.69	19.85
$\|v\|_{max}$ (ms^{-1})	19.85	23.76	25.32	22.93	20.36
Y (km)	−1950	−2250	−2100	−2250	−2100

The results denote that orography has the capacity to raise the intensity of the LLJ, and the higher as well as the steeper the orography, the more effectively the topography exerts on the LLJ. Integrating to 12 hr. the magnitude of u component, the peak value of the total wind velocity and the horizontal distance from the right boundary for the five experiments are enumerated in Table 2. It is evident that orography draws the wind center near the sloped topography. Figs.10 and 11 show the distribution of the total wind velocity at 12 hr. for the experiments (1) and (2) respectively. Fig.12 depicts the distribution of the difference of the total wind velocity at 12 hr. between with and without topography, from which it appears that the impact of the topography on the wind velocity exhibits spatially as a wave form, the nearer the sloped topography, the larger is the wave amplitude. Of course, for small topography, the influence on the LLJ is certainly not so evident.

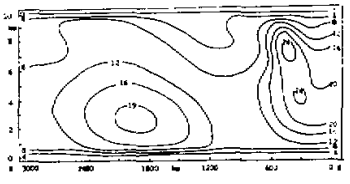

Fig.10. y−z cross section of the total wind velocity at $t=12$ hr. and without topography. unit:ms^{-1}.

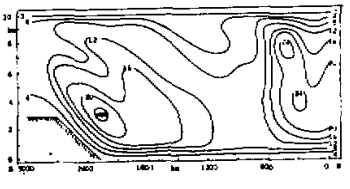

Fig.11. Same as Fig.10, except with topography.

IV. CONCLUDING REMARKS

From the foregoing application of the two dimensional reductive perturbation method to the dynamic study of the LLJ and the numerical results thereof, we come to conclusions that:

(1) The multiple dimensional reductive perturbation method and cubic Schrodinger equation are effective means for investigating the nonlinear meso−scale weather system. If the wave of shallow water can be recognized mathematically as the wave solution of elliptical function with invariable form derived from the one−dimensional KDV equation, then it is

more admissible to consider the mesoscale system with strong dispersive characteristics as the non-linear cubic Schrodinger envelope solitary wave of the cubic Schrodinger equation, because that to consider the many meso-scale system of the real atmosphere as the solitary wave with unchangeable form is clearly unreasonable. Meanwhile the preliminary study indicates that there does not exist solitary wave solution of cubic Schrodinger equation with invariable form.

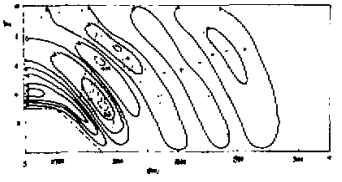

Fig.12. y-z cross section of the difference of the total wind velocity at 12 hr. between with and without topography. shaded areadenotes-positive value.

(2) The genesis of the LLJ is investigated by means of numerical integration of the cubic Schrodinger equation. The results demonstrate that LLJ is generated through the downward transfer of momentum in conjunction with the impedance of the ground surface so as to concentrate the horizontal momentum in the layer between about 850 and 700 hPa. If the topography of the underlying surface is noticeable, it can contribute to horizontal position of the LLJ. Moreover, inertia-gravity internal wave plays fundamental role in the process of formation of LLJ, and the initial wind field is important as well.

(3) The comparison between the linear and non-linear experiments denotes that the non-linear interactin has significant impact on the genesis of LLJ, nonetheless its cntribution to the LLJ is different in different environmental field. Turbulent viscosity is unfavorable for or delays the formation of the LLJ. A moderate orography has influence not only on the intensity of the LLJ but also on its position. Of course, in our experiment the impact of the diminutive topography is slight.

However, the reduction perturbation method has restriction in itself. It is only applicable to the weakly nonlinear wave, and useful simply in the analysis of the far field. In order to get good result to accommodate the actual problem, this method must be used in combination with other methods.

REFERENCES:

Chen,Q.S. (1982), The instability of the gravity-inertia wave and its relation to low level jet and heavy rainfall, *J.Meteo.Soc.Japan.*, **60**: No.5, 1041-1057.

Gao Shouting, Sun Shuqing (1984), The Forming of Subsynoptic Scale Low Level Jet Stream. *Scientia Atmospherica Sinica*, **8**: 178-188.

Hart,J.E. (1977), On the theory of the East African lowlevel jet stream, *Pageoph*, **115**: 1263-1282.

Lin Biyuan (1988), The History and the Current Situationof the Mesoscale Meteorological Research, *Qixiang Keji*, **1**: 1-6.

Ninomiya,K.,and Akiyama,T. (1974), Band structure of mesoscale echo clusters associated with low leveljet stream, *J. Meteor. Soc. Japan.*, **52**: 300-313.

Pedlosky,J. (1979), Introduction to the Geophysical Fluid Dynamics.

Synoptic Section of the Tropical Oceanographic and Meteorological Institute of Guangdong Province (1977), The Low Level Jet Process and the Analysis of Heavy Rainfalls of Guangdong Province during Its Earlier Flood Season, *Scientia Atmospherica Sinica*, **2**: 99–104.

Uccellini,L.W.,and Johnson, D.R. (1979), The coupling of upper and lower tropospheric jet streaks and implications for the development of severe con vective storms, *Mon. Wea. Rev.*, **107**: 682–703.

Yang Dasheng (1983), The Preliminary Study of the Dynamicsof the Large Scale Low Level Jet, *Acta Oceanologica Sinica*, **5**: 434–445.

Yang Dasheng, Zhang Zuojun, (1984), The Response of the LargeScale Low Level Jet to the Boundary Conditions, *Acta Scientiarum Naturalum Universitatis Pekinensis* **6**: 45–58.